Experimental Investigation of Spray Characteristics of Electro-Hydro-Dynamic Atomization

Shehzaib Yousuf Khan, Muhammad Uzair*, Usman Allauddin, and Assaad Marsi

***Abstract*—** *Electrostatically charge injection atomization of Fatty Acid Methyl Ether (FAME) called Biodiesel is shown to work varying electrode gap to diameter ratio and injection velocities. An experimental setup has been built for observing the break-up mechanism of Biodiesel sprays against Diesel. The electrohydrodynamics (EHD) atomization is found to be a workable method to generate quality sprays for small internal combustion engines. In this study, an atomizer similar to a third-generation charge injection atomizer with a plane-to-plane electrode was designed and manufactured at The University of Sydney. The spray characterization is used in both macroscopic and microscopic aspects with dual-angle Particle Tracking Velocimetry technique with imaging mode and image processing with CMOS camera respectively. The breakup length, location of on-set of dispersion, and spray angle were measured for different operating conditions with different interelectrode gap and injection velocity by increasing the applied voltage supplied from the power source.*

***Keywords*— Electrohydrodynamic; spray characterization; atomization; Biodiesel; breakup length; on-set location.**

1. INTRODUCTION

The Electrostatic atomization of liquid fuels has always been a significant topic for combustion for past four decades where Kim & Turnbull used a chemically etched tip needle in a glass capillary with very low flow rates and current to produce electrostatic spraying in insulators [1]. Due to dearth of knowledge on EHD atomization, the commercial use of it is limited in combustion process. The mechanism of EHD atomization is similar to the fuel injection system in small IC engines; however EHD is promising and efficient technique in small eninges (50-100cc) and micro combustor to produce fuels spray consuming very low electrical power (~ 2mW). The technology was matured time to time by the improved designs of EHD atomization. The first version design was equipped with s simple electrode [2,3] followed by the second-generation design of Kelly [4]. Kelly proposed a modified atomizer 'Spray Triode', by providing an additional grounded electrode. The similar work was performed by some other researchers [5,6,7] to improve the performance. In third version, Shrimpton [8,9,10] improved the performance by adding co-axial alignment of electrode tip and nozzle orifice. The EHD atomization is still under great research and to improve the performance, the stainless-steel sewing needle was used by Yule et. al [11] of tip radius 60 μm which corrected the wrong assumption of Kelly [2] based on the field emission mechanism of Kim & Turnbull [1], that Spray Triode required emitter tip radius of less than 1 μm so that the surface electric field intensity is increased. Shrimpton [9,10] preferred to use negative polarity over positive. The charge emitting electrode requires lower electric field intensities E ~ 5 x10^9 V/m for negative polarity or field emission, whereas positive polarity or field ionization typically requires E ~ 5 x 10^{10} V/m, greater in magnitude of 10, which was proposed by Robinson et al [12]. Crowley [13] suggested that the electric breakdown strength in most of the commercial fuels is found to be E ~ 20 x 10^6 V/m. There was an effort made on laboratory scale to examine the use of charged water drop with atomization [14]. The purpose was to propose the new method to remove particles to avoid the previously used traditional methods of water film and mechanically atomized spray. Electrohydrodynamic atomization, the cost-effective technology [15, 16], provides the advantage to utilize the processing of numerous materials [17,18]

The main objective of this paper is to find out the spray characteristics of EHD atomization using third generation type atomization in the primary region where the jet breakup is observed. The atomization can be induced by the electric repulsive force which is proportional to the electric charge, also the electro-convective turbulence is promoted potentially which is as efficient as compared to pressure atomization. The dielectric nature of Diesel and Biodiesel carries the electric charge causing dispersion and breakup of injected fluid into fine spray and droplets due to disruptive electric field. The spray characteristics are defined by the quality of atomization which include finer droplet, larger cone angle of sprays and shorter jet breakup length. The quality of spray is always desired with parameters such as jet breakup length, breakup angle and droplet size. The breakup length is the distance from the nozzle orifice to the breakup of the liquid jet.

Shehzaib Yousuf Khan is with School of Aerospace, Mechanical and Mechatronic Engineering, The University of Sydney, Australia.

Muhammad Uzair, Usman Allauddin are with Department of Mechanical Engineering, NED University of Engineering and Technology, Pakistan.

*Corresponding author: Muhammad Uzair; Email: uzair@neduet.edu.pk.

2. EXPERIMENTAL SETUP

The electrohydrodynamic (EHD) atomization was performed using pulsed charge injection atomizer. The atomizer was completely fabricated at The University of Sydney. The main parts of the atomizers were (a) Perspex based atomizer and electrode housing, (b) Copper bases electrode and orifice base disk and (c) micrometer. The orifice disk, also known as grounded electrode, had a central nozzle of 250 μm diameter (D). Starrett 262RL Micrometer was used to adjust the inter-electrode gap (L) from electrode tip to the orifice disk. The non-rotating spindle of micrometer has the setting range from 0 to 1 inch with 0.001-inch graduation. The inter-electrode gap was selected at different positions (8, 10, 12, 15, 17, 19, 21, and 23) to capture the significant normalized electrode gap (the ratio of electrode gap to diameter of nozzle (L/D)). The atomizer was used to inject an electrostatic charge to produce jet breakup and spray. The charge was passed through the nozzle orifice.

The schematic of Electrohydrodynamic atomizer is shown in Figure 1. The high voltage power supply (Spellman SL Series; model SL10) was used to provide the required potential difference. In order to conduct the experiments, two different configurations of hydraulic fuel circuit were set. In one setup, the simple control valve was provided along with the float connected to pressurized cylindrical vessel. While there were two syringe pumps coupled in parallel in second configuration (Figure 1). The fuel was supplied from fuel drum with oil filter and pressure tees and valves connected to filter contaminants and control the capacity of the syringe. The micro-meter and pico-meter were installed to measure the leakage current I_L and spray current I_S respectively. In order to provide a continuous and steady flow through hydraulic circuit and the atomizer nozzle orifice, 40 psi pressure cylinder was set. The flow rate was controlled initially with simple flow control float value which was directly connected with a pipe to the atomizer fuel inlet. The flow control valve was calibrated for flow rates with float. The operating condition for Diesel fuel was obtained at flow rate of level 6 giving 9.31 mL/min of volumetric flow rate for constant nozzle diameter D=250μm and injected velocity $uinj$ = 3.4 m/s. Later on, the GenieTouch syringe pump system was used consisting of two syringes at a time facing same direction with capacity up to 60ml. The flow rates were calibrated for different injected velocity $uinj$ = 2.5, 5, 7.8 and 10 m/s and constant nozzle diameter D=250μm giving volumetric flow rates of 7.36, 14.73, 22.90, 29.35 mL/min.

Table 1 represents the properties of 5 different fuels used to perform the experiments on EHD atomization. The Biodiesel blends B1, B2, B3 and B4, having different carbon chain lengths and saturation levels, are the fatty acid methyl esters (FAMEs) produced from methanolysis transesterification of Palmere, Coconut, Pale and Canola Oils respectively [19,20]. B4 is almost fully unsaturated and have long and similar chain lengths to B3 as compared to B1 and B2, however B3 is partially unsaturated. B1 and B2 are saturated FAMEs where B2 has shorter carbon chain length as compared to B3 and B4 while B1 has the shortest carbon chain length among all four Biodiesels. The carbon chain length affects the fuel properties such as viscosity where larger chain lengths and large molecules are highly viscous thus also resulting in lower ionic mobility which is inversely proportional to the viscosity according to Walden's rule $\kappa = C\mu\text{-}1$ [21]. The early abbreviation used for B1, B2, B3 and B4 are C810, C1214, C1618, and C1875 respectively [20].

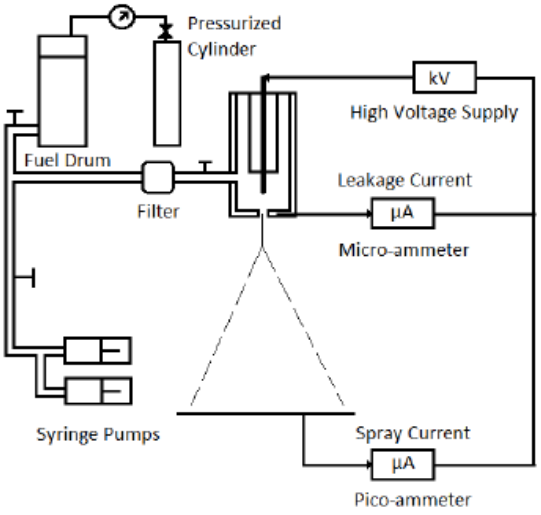

Fig. 1. Circuit Schematics of EHD Atomizer.

Table 1. Fuel Properties for the fuels [20]

Fuel Properties	B1	B2	B3	B4	Diesel
Average # of C atoms	9.5	14.8	18.3	18.7	-
Average # of H atoms	19.7	28.3	35.3	35.3	-
Relative density, (kg/m^3)	0.877	0.871	0.873	0.879	0.848
Viscosity, [Pa.s].10^3	1.71	3.81	4.32	4.65	3.2
Surface Tension, [N/m].10^3	26.1	28.4	29.9	29.96	23.0

The electrostatically charged sprays start forming by increasing applied voltage using high voltage power supply. The macroscopic aspect of charged sprays was observed and recorded for spray cone angle (α) and location of onset of dispersion (x) while the microscopic level information was obtained for jet breakup location. The macroscopic structure was captured using two different CMOS cameras Canon 600D and Canon 70D with different lenses. Initially Canon 70D was used with Canon EF-S lens of focal length 50 mm and maximum aperture f/1.4, for capturing macroscopic images of atomization of Diesel fuel with L/D = 2.35, injected velocity of $uinj$ = 3.4 m/s, and applied voltage of 0, 7, 8 and 9 kV, as shown in Figure 2.

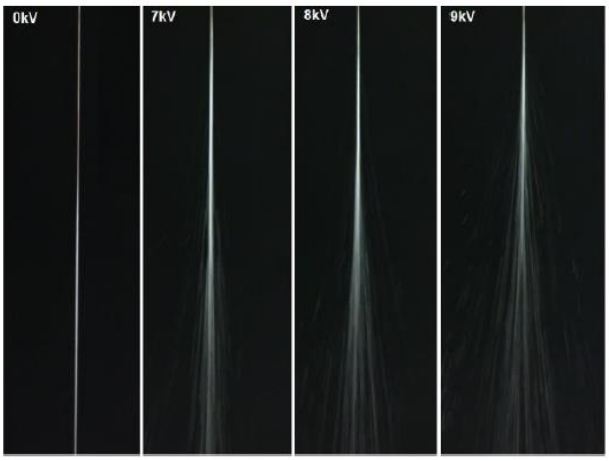

Figure 2: Macroscopic images of sprays of diesel at L/D=2.5, *uinj* = 3.4 m/s, applied voltage of 0, 7, 8 and 9 kV.

Later on, two lenses were used with Canon 600D, Tamron 17-50mm lens of focal length set at 24 mm and maximum aperture of f/2.8 and Canon EF-S lens of focal length 50 mm and maximum aperture f/1.8. The macroscopic images were obtained for sprays of Diesel and different Biodiesel blends B1, B2, B3 and B4 at different L/D ratios 1.5 and 2 and various injected velocities u_{inj}= 2.5, 5, 7.8 and 10 m/s.

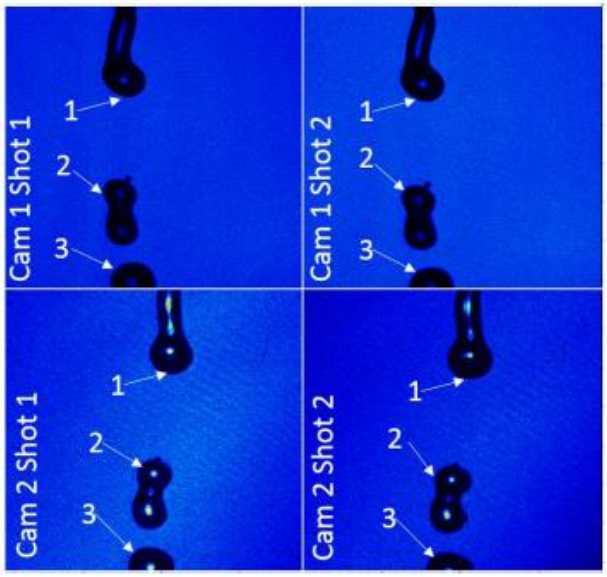

Fig. 3. An example imaging set of four 2D-images using particle tracking velocimetry technique, (#1 liquid jet tip, #2 & #3 fragments) at L/D=2.5, *uinj* = 3.4 m/s, applied voltage of 10kV.

The microscopic aspect of atomization was captured using dual angle particle tracking velocimetry (PTV) technique to measure the liquid jet breakup length under particle imaging velocimetry (PIV) mode as reported in [22]. The PTV technique is synchronised using a LaVISION high-speed controller with two lasers, two lenses and two cameras [22]. The field of view of 3.15 mm, is the same for both cameras with a spatial resolution of 4.1 μm/pixel. The two cameras capture two different images at two different time intervals t1 and t2 to obtain a set of four 2D-images. The Figure 3 shows an example of the imaging set in which one realization is captured by two cameras where images from first camera can be referred as front view of liquid jet breakup and the second as side view. This technique can be used to obtain the delay time dt= t2-t1 for the calculation of droplet velocity from the locations of fragments, and also the jet breakup length.

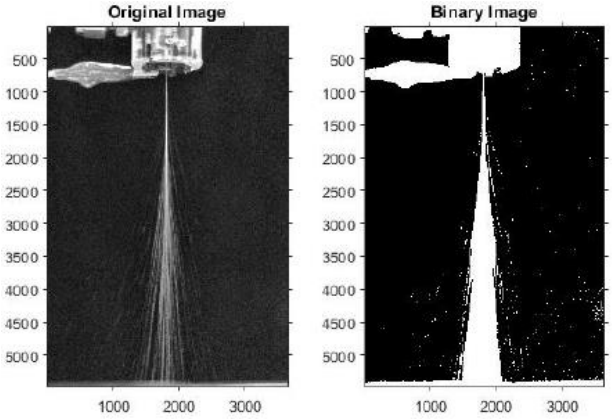

Fig. 4. Binary image of a sample image of EHD atomizer.

The image processing was done using a MatLab code to generate binary image, shown in Figure 4 and using point picking technique on the images captured using CMOS camera to determine the location of on-set of dispersion and spray cone angle α. The location of on-set of dispersion or start of dispersion is where the spray starts to separate from the injected liquid stream and spread an area. It has been observed that this location on-set of dispersion is same as jet breakup length. However, the breakup length cannot be accurate on macroscopic images due to low image resolutions that limit the visibility of jet breakup. The jet breakup length can only be measured using microscopic images captured using particle tracking velocimetry technique and an image processing script.

3. RESULTS

The macroscopic images captured using CMOS camera and applying image processing code in MatLab, the locations of on-set or start of dispersion and spray angles were determined. While the microscopic imaging from particle tracking velocimetry technique determined the jet breakup length. The probability density of the vertical point of the liquid jet tip is shown in Figure 5 at different applied voltages of 0, 7, 8 and 10 kV. The peak value for each condition was obtained and recorded for jet breakup length which is also the standard deviation of the probability density of axial locations of jet tip.

The PD of axial locations of jet tips was observed to be wider consistently for higher voltages which were due to the higher charge causing repulsive electric field that interplay with the surface tension force. The peak values of PD as the jet breakup length values are shown in Figure 6 comparing the location of on-set of dispersion and spray cone angle. As applied voltage increased the spray cone angle increased, however the jet breakup

length showed similar behaviour as the location of on-set of dispersion it was smaller numerically. This is because the macro structure of atomization was not good enough to identify the jet breakup tip location. The spray angle significantly increased with voltage is comparable with Shrimpton and Yule [24-25], Rigit [26-28] and Malkawi [30] models; this is due to the strong repulsive electric field between the surface and the tip of liquid jet. The locations of on-set of dispersion were determined using image processing technique and plotted with increasing the applied voltage at D=250µm, L/D=1.5 and 2 with different injection velocities uinj=2.5, 5, 7.8 and 10 m/s as shown in Figures 7, 8, 9, 10 and 11 respectively.

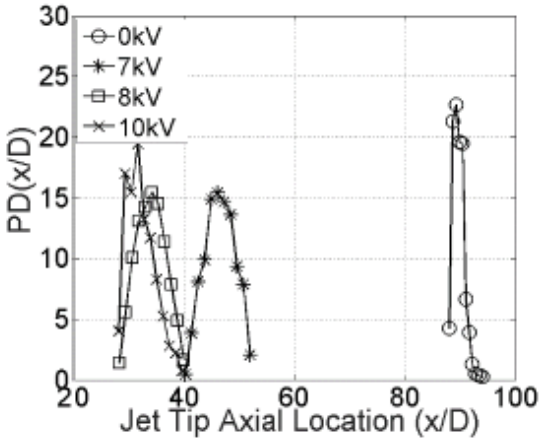

Fig. 5. Probability density of axial location (x/D) of liquid jet tip at L/D=2.5, D=250µm and uinj=3.4m/s.

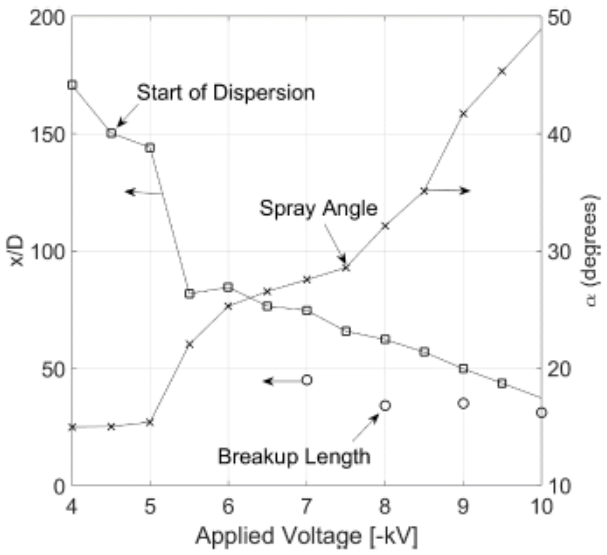

Fig. 6. Effect of increasing applied voltage on the location of on-set of dispersion, jet breakup length and spray angle.

The theoretical values of jet breakup length can be determined by substituting the values provided in the table 2 for Diesel and different Biodiesel blends. The constant C in ionic mobility is determined from the experimental data by substituting the fuel properties and which is approximated by taking median as shown in Table 6.1. The constant C is similar to the Castellanos approximation [19,20] for ionic mobility ~ 3×10^{-11} for diesel fuel while for lower viscosity biodiesels there are large differences and much smaller values than the higher viscous fuels.

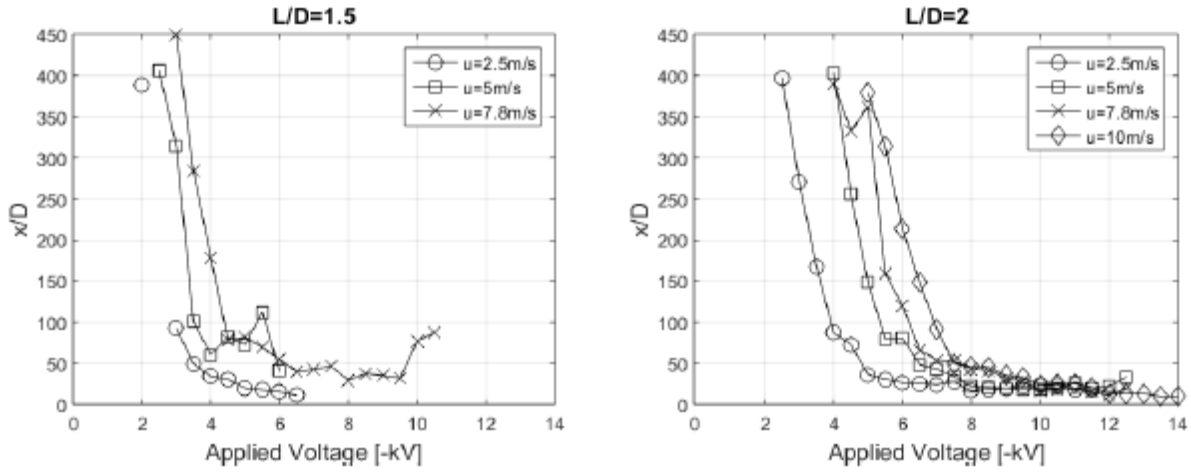

Fig. 7. x/D versus voltage for Diesel at D=250µm, L/D=1.5 and 2 with different injection velocities uinj=2.5, 5, 7.8 and 10 m/s.

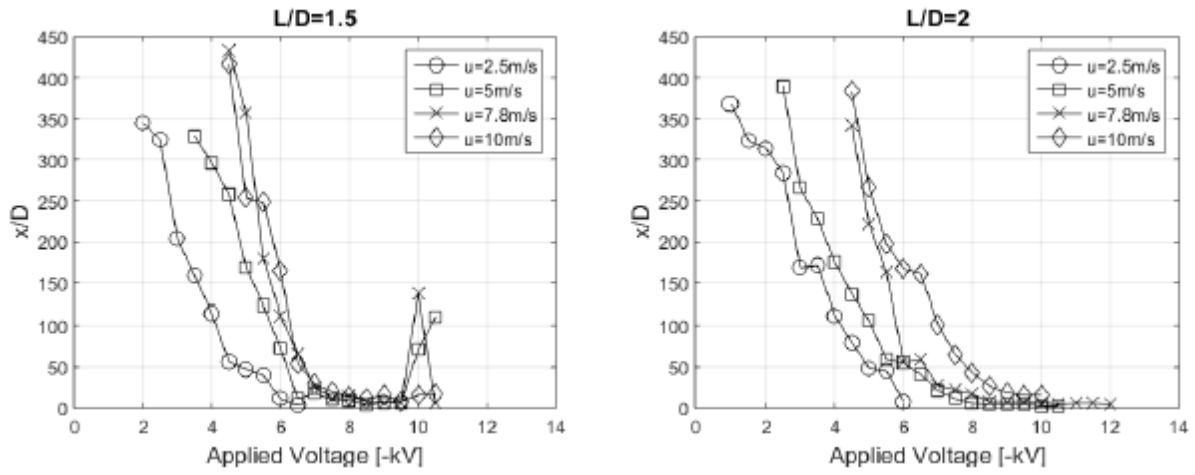

Fig. 8. x/D versus applied voltage for Biodiesel B4 at D=250µm, L/D=1.5 and 2 with different injection velocities uinj=2.5, 5, 7.8 and 10 m/s.

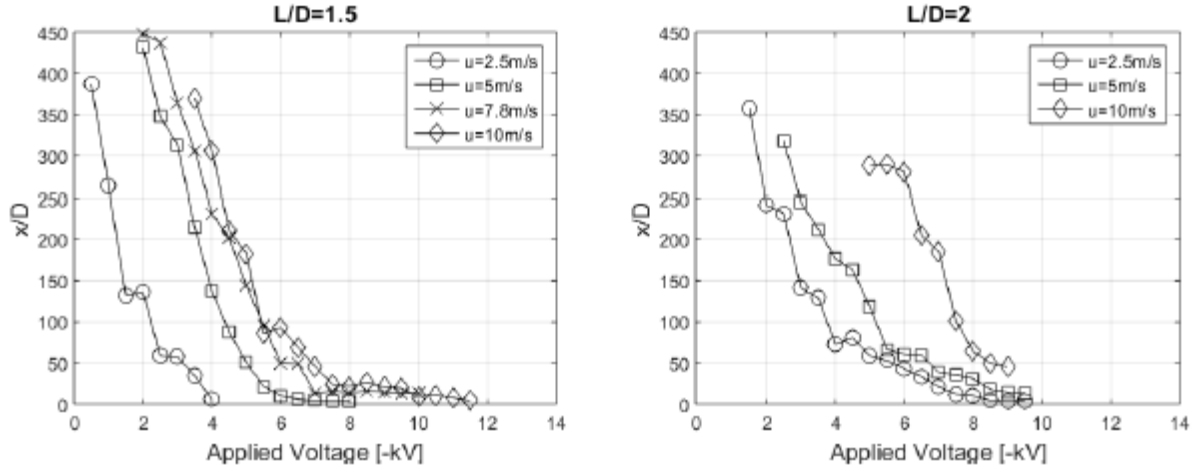

Fig. 9. x/D versus voltage for Biodiesel B3 at D=250µm, L/D=1.5 and 2 with different injection velocities uinj=2.5, 5, 7.8 and 10 m/s.

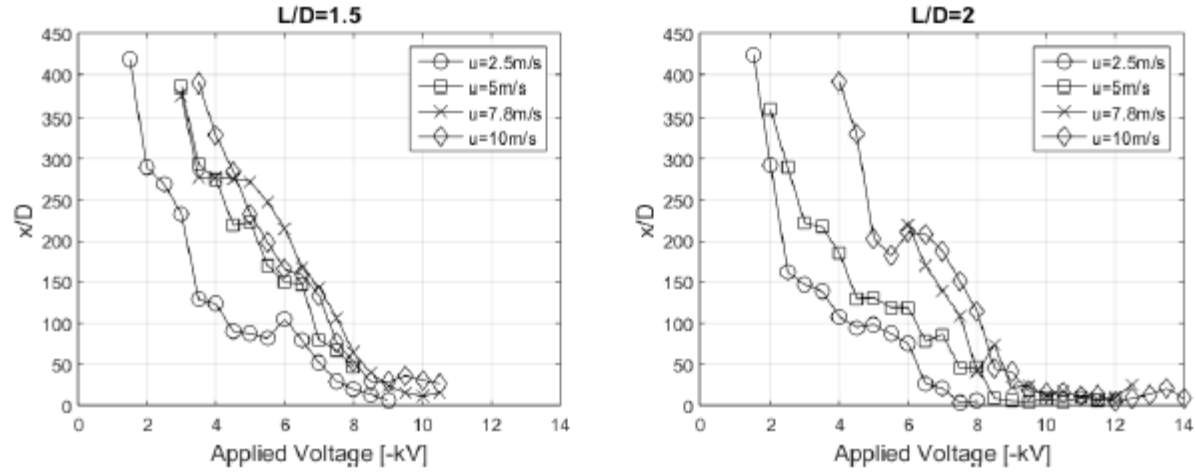

Fig. 10: x/D versus voltage for Biodiesel B2 at D=250µm, L/D=1.5 and 2 with different injection velocities uinj=2.5, 5, 7.8 and 10 m/s.

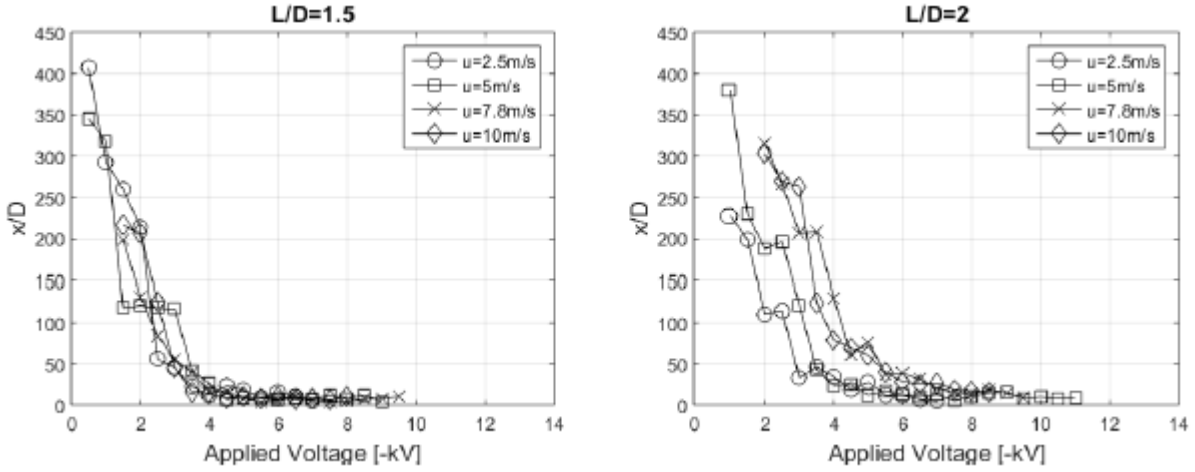

Fig. 11. x/D versus voltage for Biodiesel B1 at D=250µm, L/D=1.5 and 2 with different injection velocities uinj=2.5, 5, 7.8 and 10 m/s.

Table 2: Operating conditions for breakup length correlation for Diesel and different Biodiesel blends

Fuel	C	K (Ns/m^2)	Qv (C/m^3)	Vo (-kV)
B1	2.05 × 10-10	1.20 × 10-7	0.1 – 0.33	1
B2	1.19 × 10-10	3.12 × 10-8	0.11 – 0.56	2.5
B3	4.74 × 10-11	1.10 × 10-8	0.21 – 0.58	3.5
B4	3.59 × 10-11	7.72 × 10-9	0.2 – 0.76	3.5
Diesel	3.00 × 10-11	9.38 × 10-9	0.23 – 0.78	2.5-4

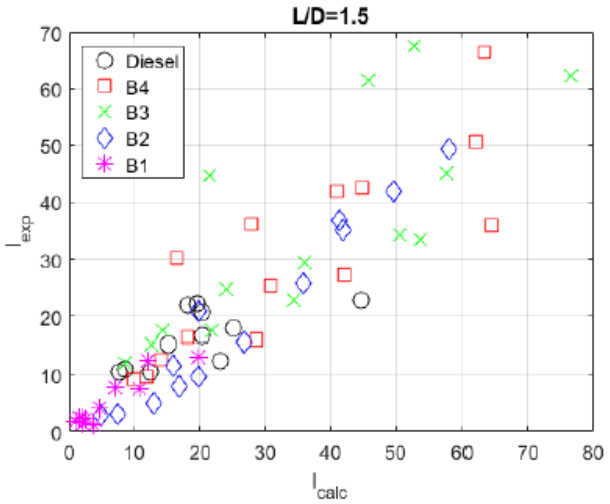

Figure 12: Experimental versus theoretical breakup length for Diesel and Biodiesel blends B1, B2, B3 and B4 at D=250µm and L/D = 1.5 with uinj=2.5, 5, 7.8 and 10 m/s

The experimental breakup length is taken as the location of the on-set of spray with a range of spray specific charge Qv as shown in Table 2. The Figures 12 and 13 show the results for experimental values of breakup length versus theoretical values for different biodiesels B1, B2, B3 and B4 in comparison with conventional diesel fuel. The values were found to be similar and correlation form a linear profile however for lower breakup length when the breakdown reached the values were inconsistent. Also, below the threshold voltage when breakup started dispersion, the measured values did not match with the theoretical value. This was because the locations of on-set of dispersion were taken as experimental breakup length where jet breakup cannot be identified. The jet breakup angle or spray cone angle versus applied voltage for variable jet velocities of u = 2.5, 5, 7.8 and 10 m/s at L/D = 1.5 and 2 are plotted in Figures 14-18. The angle profile reaches a peak value and drops. As the applied voltage increases the spray cone-angle becomes larger and for higher jet velocities the spray angle narrows down.

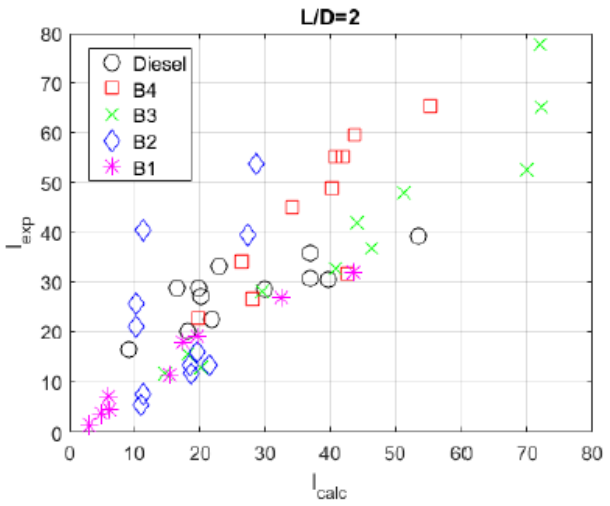

Figure 13: Experimental versus theoretical breakup length for Diesel and Biodiesel blends B1, B2, B3 and B4 at D=250µm and L/D = 2 with uinj=2.5, 5, 7.8 and 10 m/s.

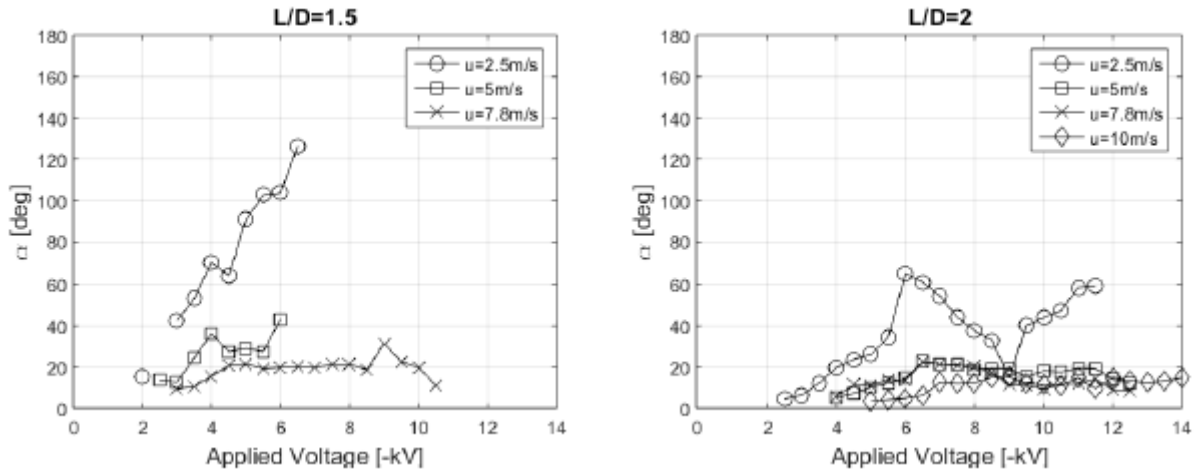

Fig. 14. Breakup angle versus voltage for Diesel at D=250µm, L/D=1.5 and 2 with different injection velocities uinj=2.5, 5, 7.8 and 10 m/s.

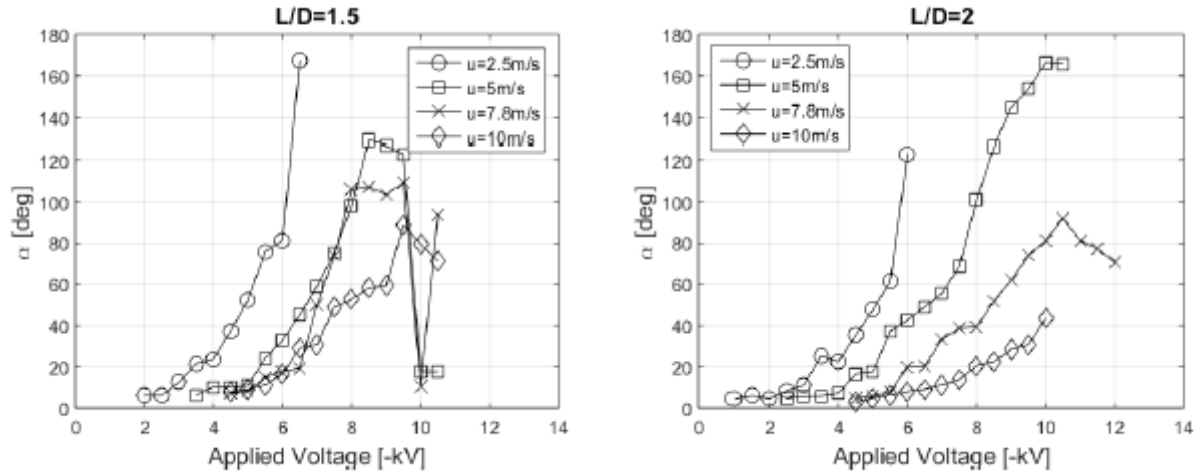

Fig. 15. Breakup angle versus voltage for Biodiesel B4 at D=250µm, L/D=1.5 and 2 with different injection velocities uinj=2.5, 5, 7.8 and 10 m/s.

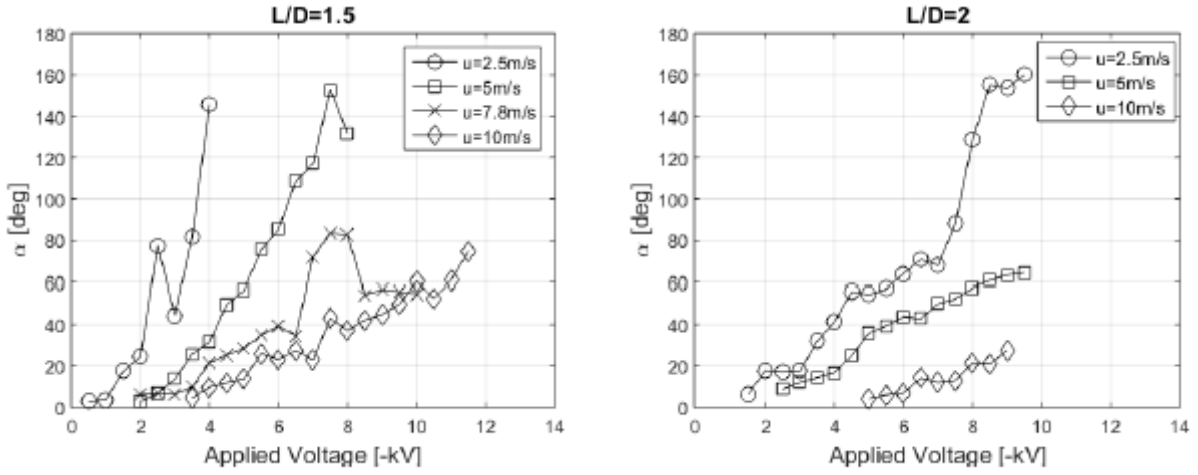

Fig. 16. Breakup angle versus voltage for Biodiesel B3 at D=250µm, L/D=1.5 and 2 with different injection velocities uinj=2.5, 5, 7.8 and 10 m/s.

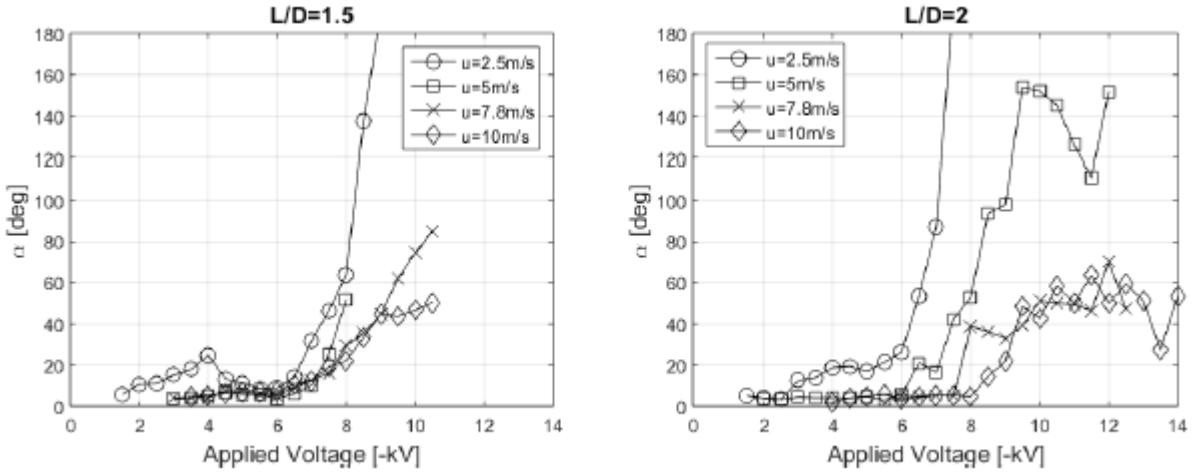

Fig. 17. Breakup angle versus voltage for Biodiesel B2 at D=250µm, L/D=1.5 and 2 with different injection velocities uinj=2.5, 5, 7.8 and 10 m/s.

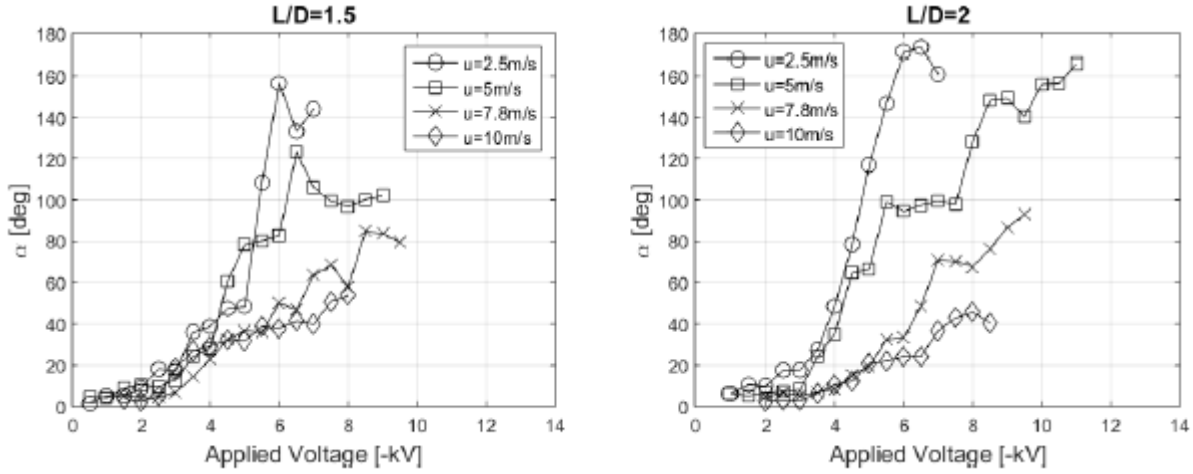

Fig. 18. Breakup angle versus voltage for Biodiesel B1 at D=250µm, L/D=1.5 and 2 with different injection velocities uinj=2.5, 5, 7.8 and 10 m/s.

4. CONCLUSION

The Diesel and Biodiesel sprays in the Electrostatically charged injection system have been experimentally investigated and the results from this study prove that the electric charge is significant in measuring the break-up length. The injection velocity is also significant and for higher values, the break-up length increases. The spray angle increases with increasing the voltage and reaches a critical value then start decreasing slowly. The location of the onset of dispersion spray is relative to the break-up length which varies with applied voltage for all biodiesel blends similar to commercial diesel. To achieve a better quality of spray the specific charge and leakage current are relatable. The specific charge should be maximum to obtain a large spray angle and a smaller jet breakup length. Also, the leakage current provides the operating conditions like threshold voltage where the higher viscous fuels have better specific charges i.e. higher.

ACKNOWLEDGEMENTS

We would like to thank The University of Sydney for giving the opportunity to research in the field of Electrohydrodynamics.

REFERENCES:

[1] Kim, K., Turnbull, J.: Generation of charged drops of insulating liquids by electrostatic spraying. Journal of Applied Physics 47(5), 1964 (1976)
[2] Jido, M.: Study of Electrostatic Charged Droplets: Part 1. J. Jap. Soc. Chem. Eng. 40, 24–33 (1986)
[3] Jido, M.: Study of Electrostatic Charged Droplets: Part 2. J. Jap. Soc. Chem. Eng. 41, 32–40 (1987)
[4] Kelly, A.J.: The electrostatic atomization of hydrocarbons. Journal of the Institute of Energy, 312–320 (June 1984)
[5] Alj, A., Denat, A., Gosse, J.P., Gosse, B.: Creation of charge carriers in non-polar liquids. IEEE

Transaction on Electrical Insulation 20(2), 221 (1985)
[6] Denat, A., Gosse, J.P., Gosse, B.: Electrical Conduction of Purified Cyclohexane in a Divergent Electric Field. IEEE Transactions on Electrical Insulation 23(4), 545–554 (1988)
[7] Nemamcha, M., Gosse, J.P., Gosse, B., Denat, A. Influence of insulating electrode coatings on the electrical conduction of cyclohexane. IEEE Transaction on Electrical Insulation 23(4), 529 (1988)
[8] Shrimpton, J.S, Charge Injection System, Springer 2009
[9] Shrimpton, J.S.: Electrostatic Atomization and Combustion of Hydrocarbon Oils, PhD thesis, UMIST, Manchester, UK (1995)
[10] Shrimpton, J.S.., Electrostatic Atomization and Combustion of Hydrocarbon Oils. UMIST, 1995.
[11] A.J. Yule, J.S. Shrimpton, A.P. Watkins, W. Balachandran, and D. Hu. Electrostatically atomized hydrocarbon sprays. Fuel, 74:10941103, (1995).
[12] Robinson, K. S., Turnbull, R. J., and Kim, K., "Electrostatic Spraying of Liquid Insulators," Trans. IEEE Ind. App. Sys. 16: 308-317, 1980.
[13] J.M. Crowley. Fundamentals of Applied Electrostatics. Laplacian Press, 1999.
[14] Teng C, Fan X, Li J. Effect of charged water drop atomization on particle removal performance in plate type wet electrostatic precipitator. Journal of Electrostatics. 2020
[15] S. Jayasinghe, M. Edirisinghe, D. Wang, Controlled deposition of nanoparticle clus-ters by electrohydrodynamic atomization, Nanotechnology 15 (2004) 1519.
[16] N. Bhardwaj, S.C. Kundu, Electrospinning: a fascinatingfiber fabrication technique,Biotechnol. Adv. 28 (2010) 325–347
[17] Z. Ma, M. Kotaki, R. Inai, S. Ramakrishna, Potential of nanofiber matrix as tissue-engineering scaffolds, Tissue Eng. 11 (2005) 101–109
[18] S.J. Hardman, N. Muhamad-Sarih, H.J. Riggs, R.L. Thompson, J. Rigby, W.N. Bergius,L.R. Hutchings, Electrospinning superhydrophobicfibers using surface segregatingend-functionalized polymer additives, Macromolecules 44 (2011) 6461–6470
[19] P.X. Pham. A. Kourmatzis and A.R. Masri, 20th Australasian Fluid Mechanics Conference, Perth, Australia Dec. 2016
[20] P.X. Pham . Influences of Molecular Profiles of Biodiesels on Atomization, Combustion and Emission Characteristics. PhD Thesis, The University of Sydney, Sydney, Australia (2015)
[21] Chang, J. S., Crowley, J. M., and Kelly, A. J., "Handbook of Electrostatic Processes. Dekkar," 1995.
[22] P.X. Pham. A. Kourmatzis and A.R. Masri, 20th Australasian Fluid Mechanics Conference, Perth, Australia Dec. 2016
[23] J.S. Shrimpton and A.J. Yule, Experiments in Fluids, 26(5) (1999) 460-469
[24] Shrimpton, J. S. and Yule, A. G., "Atomization, Combustion and Control of Charged Hydrocarbon Sprays," Atomization and Sprays 11: 365–396, 2001.
[25] Shrimpton, J. S., and Yule, A. J., "Electro-hydrodynamics of Charge Injection Atomization: Regimes and Fundamental Limits," Atomization and Spray 13:173-190, 2003.
[26] Rigit. A.R.H. Performance of a Charge Injection Electrostatic Atomizer and Spray Characteristics. Imperial College London, 2003.
[27] Rigit, A.R.H.: performance of a charge injection atomizer and spray characteristics, PhD thesis, University of London (2005)
[28] Rigit, A. R. H. and Shrimpton, J. S., "Spray Characteristics of Charge-injection Electrostatic Atomizers with Small-Orifice Diameters," Atomization and Sprays 16:421–442, 2006.
[29] G. Al-Ahmad, J.S. Shrimpton, E.L. Ergene and F. Mashayek, Atomization and Sprays, 19(6) (2009) 547-566
[30] G. Malkawi. Point-to-plane and plane-to-plane electrostatic charge atomization for insulating liquids. University of Illinois at Chicago, 2010.